NASA Technical Memorandum 100254
AIAA-88-0263

Noise of a Model Counterrotation Propeller With Reduced Aft Rotor Diameter at Simulated Takeoff/Approach Conditions (F7/A3)

Richard P. Woodward
Lewis Research Center
Cleveland, Ohio

and

Eliott P. Gordon
Sverdrup Technology, Inc.
Lewis Research Center
Cleveland, Ohio

Prepared for the
26th Aerospace Sciences Meeting
sponsored by the American Institute of Aeronautics and Astronautics
Reno, Nevada, January 11-14, 1988

NASA

NOISE OF A MODEL COUNTERROTATION PROPELLER WITH REDUCED AFT ROTOR DIAMETER AT SIMULATED TAKEOFF/APPROACH CONDITIONS (F7/A3)

Richard P. Woodward
National Aeronautics and Space Administration
Lewis Research Center
Cleveland, Ohio 44135

and

Eliott B. Gordon
Sverdrup Technology, Inc.
Lewis Research Center
Cleveland, Ohio 44135

E-3880

SUMMARY

A model high-speed advanced counterrotation propeller, F7/A3, was tested in the NASA Lewis Research Center's 9- by 15-Foot Anechoic Wind Tunnel at simulated takeoff/approach conditions of 0.2 Mach number. Acoustic measurements were taken with an axially translating microphone probe, and with a "polar" microphone probe which was fixed to the propeller nacelle and could take both sideline and circumferential acoustic surveys. Aerodynamic measurements were also made to establish propeller operating conditions. The propeller was run at two blade setting angles (front angle/rear angle) of 36.4°/43.5° and 41.1°/46.4°, forward rotor tip speeds from 165 to 259 m/sec (540 to 850 ft/sec), rotor spacings from 8.48 cm (3.34 in.) to 14.99 cm (5.90 in.) based on pitch change axis separation, and angles of attack to ±16°. The aft rotor diameter was 85 percent of the forward rotor diameter to reduce tip vortex-aft rotor interaction as a major interaction noise source. Results are compared with equal diameter F7/A7 data which was previously obtained under similar operating conditions. The aft rotor-alone tone was 7 dB lower for the reduced diameter aft rotor, due to reduced tip speed at constant rpm. Interaction tone levels for the F7/A3 propeller (compared to the F7/A7 propeller) were higher at minimum blade row spacing and lower at maximum spacing.

INTRODUCTION

Modern high-performance turboprop aircraft offer the promise of considerable fuel savings while still allowing for a cruise speed similar to that of current turbofan aircraft. Advanced counterroration propellers may offer from 8 to 10 percent additional fuel savings over similar single rotation propellers at cruise conditions (ref. 1). However, there is considerable concern about the potential noise generated by such aircraft, which includes both in-flight cabin noise and community noise during takeoff and landing.

This paper presents the acoustic results for a model counterrotation propeller which was tested in the NASA Lewis 9- by 15-Foot Anechoic Wind Tunnel. The test results are for 0.20 Mach, which is representative of takeoff/approach operation. The test propeller (designated F7/A3) had 11 forward and 9 aft blades. The aft propeller had a smaller diameter than the forward propeller

to reduce its interaction with the forward propeller tip vorticies. This interaction is thought to be a major contributor to the noise of counterrotation propellers (refs. 2 and 3). Selected results will be compared with those for the F7/A7 propeller (ref. 4) which was likewise tested at similar conditions in the Lewis 9- by 15-foot tunnel. The A7 propeller diameter was almost as great as that of the common forward propeller, F7.

The propeller was tested at three rotor spacings at fixed blade angles to investigate spacing effects, and with increased blade angle at maximum spacing to investigate loading effects. It was operated over a range of rotational speeds corresponding to forward rotor tip speeds from 191 m/sec (626 ft/sec) to 259 m/sec (850 ft/sec) and at angles of attack up to ±16°. Acoustic data were taken with a track "flyover" microphone probe which was fixed to the tunnel floor and with a "polar" microphone probe which was mounted on the downstream end of the propeller housing. This polar probe assembly moved with the model at angle of attack and surveyed both the angular and sideline noise fields.

The unequal blade numbers of the 11 + 9 configuration of the F7/A3 propeller greatly simplified the acoustic analysis of the complicated counterrotation propeller spectra. Corresponding aerodynamic results will be presented to establish the propeller operating conditions.

APPARATUS AND PROCEDURE

The NASA Lewis 9- by 15-Foot Anechoic Wind Tunnel is located in the low-speed return leg of the supersonic 8- by 6-Foot Wind Tunnel. The maximum airflow velocity in the tunnel is slightly over 0.2 Mach, which provides a takeoff/approach test environment. The tunnel acoustic treatment was recently modified to provide anechoic conditions down to a frequency of 250 Hz, which is lower than the range of the fundamental tone produced by the F7/A3 propeller.

Acoustic instrumentation in the 9- by 15-foot tunnel consisted of two remote-controlled acoustic probes, a flyover probe and a polar probe. The probes were instrumented with 0.64 cm (0.25 in.) condenser microphones. Two microphones were mounted on the "track" (or flyover) probe which was fixed to the tunnel floor, and one microphone was mounted on the "polar" probe which was attached to the aft propeller housing. Figure 1 shows the model propeller and acoustic instrumentation installed in the anechoic wind tunnel. The track translating microphone probe traversed 6.50 m (21.33 ft) which covered most of the 8.2 m (27 ft) length of the treated test section. The track probe data presented in this paper is for the inner microphone, which was located 137 cm (54 in.) from the propeller axis for 0° angle of attack. (The second microphone was located 30 cm (1 ft) ahead and 30 cm (1 ft) further out from the first microphone.) The inner microphone of the track probe surveyed sideline angles from 18 to 150° relative to the propeller axis of rotation (at 90° referenced to the aft propeller plane) with the propeller at 0° angle of attack.

The polar microphone probe had the capability to survey much of the propeller noise field. As shown in the sketch of figure 2, the polar microphone probe was mounted on the downstream propeller housing and moved with the propeller at angles of attack. The probe could perform sideline acoustic surveys

extending about 45° fore and aft of the aft propeller plane. Circumferential surveys could be made over a 240° range, being limited by support hardware interference. However, it was possible to construct complete 360° directivities by combining the results for corresponding positive and negative angles of attack. The polar probe microphone was located 61 cm (2 ft) from the propeller axis of rotation. A comparison of sideline survey results for the track and polar probes (ref. 4) showed that the polar probe measures the propeller far-field noise.

The counterrotation propeller model designated F7/A3 was used in these experiments. The front propeller is 62.2 cm (24.5 in.) in diameter, and the aft propeller is 53.1 cm (20.9 in.) in diameter (table I). The aft propeller diameter was reduced to investigate expected acoustic benefits associated with avoiding the impingement of the vortex wake of the upstream propeller on the downstream propeller. The F7/A3 results are compared to those for the equal diameter F7/A7 model propellers (ref. 4) which were tested under similar conditions in the 9- by 15-foot tunnel. Both model propellers were run in the 11 + 9 blade configuration, with blade setting angles for essentially equal torque between the two blade rows. This also resulted in a nearly equal thrust split for the test conditions. Table I also presents propeller design characteristics at a cruise condition of 0.72 Mach. Aerodynamic results for the F7/A7 8 + 8 configuration are presented in reference 5. The propeller installation in the 9- by 15-Foot Wind Tunnel was powered by two independent air turbine drives, allowing the option of different rotor speeds. In practice, the two rotors were operated at about 100 rpm difference to relieve higher test rig stress experienced with nearly equal rotor speeds.

Table II shows the propeller test conditions which are reported herein. The model was operated at propeller axis angles of attack up to ±16°. The propeller was tested at a forward blade setting angle of 36.4° (measured at 3/4 radius) and aft setting angle of 43.5° at three blade row spacings. The propeller was also tested at a higher loading blade angle of 41.1°/46.4° at the maximum blade row spacing. There is currently some question as to which blade angles and tip speeds should be chosen to minimize noise while providing the necessary takeoff thrust. Increased blade angle with a corresponding rotational speed reduction (to maintain the same thrust) may lower the propeller noise. This would suggest that the more highly-loaded blade angle may be more typical of full-scale operation. Consequently, the data analysis will use the higher-loaded condition whenever possible.

The blade row spacing is presented in terms of the physical axial spacing between the upstream and downstream blade pitch change axis. This was done to facilitate a comparison between the two propellers, F7/A3 and F7/A7. While it might be desireable to express this spacing as the upstream propeller chord divided by the aerodynamic spacing (i.e., interblade row spacing along the airflow path) it is recognized that the two propellers probably have different interaction mechanisms. The F7/A7 propeller has tip vortex-aft propeller interaction as a major noise mechanism, suggesting that spacing values should be for the propeller tip region. However, the interaction noise of the reduced aft diameter F7/A3 propeller noise is probably controlled by upstream viscous wakes, which are generated throughout the blade span.

Table III presents selected aerodynamic results for both the F7/A3 and F7/A7 propellers. The propellers were operated at corrected rotational speeds. Results are shown for the operating conditions used for the analysis is this paper.

Figure 3 shows photographic plan views of the F7/A3 and F7/A7 blading. Note that the smaller-diameter A3 blade has a corresponding chord increase to maintain the same thrust as the A7 blade (at the same rpm, but with a slightly increased A3 blade angle).

RESULTS AND DISCUSSION

All tests were performed at 0.20 tunnel Mach number. Limited aerodynamic results are presented to establish the propeller operating conditions. Acoustic results show how the propeller noise is affected by angle of attack, blade angle, tip speed, blade row spacing, and blade row numbers. Comparisons with the larger aft diameter F7/A7 configuration will show the acoustic benefits of reducing the aft propeller diameter.

Aerodynamic Performance

Figure 4 is a propeller operating map of the total power density (based on the forward propeller), PQAT, as a function of the forward propeller advance ratio, J. PQAT is defined as:

$$\frac{\text{Total Power}}{(\rho)\ (\text{rev/sec})^3\ (D^3)\ (\text{Annulas area})}$$

where ρ is the local air density, and D is the forward propeller diameter. The results in figure 4 are for the maximum blade row spacing tested. Designation of the exact "takeoff design" blade angles and rotative speed is currently in a state of flux due to trade-offs between tip speed and blade loading for optimum aeroacoustic benefits. The current estimate corresponds to a J value of about 0.87, and blade angles at or slightly above the higher-loading condition shown on figure 4.

Sound Pressure Level Spectra

The acoustic spectra for counterrotation propellers may be quite complex, consisting of both rotor-alone tone harmonics for each propeller and an array of interaction tones. Figure 5 presents a typical SPL spectra for the F7/A3 propeller. Rotor-alone tones typically show a maximum level near the propeller plane while the interaction tones are often higher at forward and aft angles. The spectra of figure 5 is for 105° from the upstream propeller axis (relative to the aft propeller plane) along a 61 cm (24 in.) sideline. The fundamental rotor-alone tones (BPF_1 and BPF_2) are clearly seen in the spectra, but the higher-order rotor-alone tones are essentially buried in the broadband. Interaction tones (such as $BPF_1 + BPF_2$) dominate the spectrum at higher frequencies.

Sideline Directivity

Figure 6 presents typical sideline directivities for several F7/A3 tone orders. All of the survey results in this paper are for a 16 Hz bandwidth. These results are for the "flyover" microphone probe at a 137 cm (54 in.) sideline distance. (Results for this probe are 7 dB lower than corresponding results for the polar microphone probe according to expected distance effects

of spherical spreading.) The rotor-alone tones (BPF_1 and BPF_2) show the expected maximum levels near the propeller plane. However, the clipped aft propeller is about 5 dB quieter than the forward propeller. Both propellers are at about the same rpm and thrust level. The noise reduction of the aft propeller is greatly influenced by the reduced tip speed, as will be discussed later in this paper. The interaction tone $BPF_1 + BPF_2$ shows a minimum value near the propeller plane and maximum levels about 40° from the propeller plane. This tendency for interaction tones for counterrotation propellers to have high levels away from the propeller plane (at takeoff speeds) has been documented in the literature (refs. 4 and 6). Reference 7 presents interaction tone directivities for F7/A7 propeller operating at cruise conditions (0.72 to 0.8 Mach). The interaction tones often peaked near the propeller plane for this high-speed operation. An apparent 100 dB broadband floor for this 16 Hz analysis (observed in sideline spectra) limited the angular extent of the rotor-alone directivities. This broadband level is probably caused by microphone "self noise."

Figure 7 shows interaction tone directivities for the flyover probe with the minimum blade row spacing. These data are for the lower blade loading condition. The first interaction tone, $BPF_1 + BPF_2$ shows a similar directivity to that seen for this tone in figure 6, although at a higher overall noise level. This directivity is typical of that for most interaction tone orders; however, the $2BPF_1 + BPF_2$ tone shows a directivity more typical of rotor-alone tones with high levels near the propeller plane.

Rotor-alone tones are strongly affected by propeller axis angle of attack (refs. 4, 8, and 9). This noise increase is associated with local changes in the propeller blade angle of attack, with the unsteady blade loading producing higher noise. The maximum noise associated with propeller axis angle of attack is often observed about 90° circumferentially ahead of the maximum blade loading of the advancing propeller.

Figure 8 presents sideline directivities for the polar microphone in the aircraft flyover plane (same circumferential position as the "flyover" probe) for several propeller angles of attack. Figures 8(a) and (b) show the rotor-alone tone directivities. The forward rotor levels (fig. 8(a)) are generally higher than those for the aft rotor (fig. 8(b)) for these blade setting angles (41.1°/46.4°). As expected, there is a strong relationship between maximum tone level and angle of attack, with the forward rotor-alone tone showing a 20 dB change over the ±16° range. It should be noted that the sideline angle is based on the aft propeller plane. Thus, at maximum blade row spacing the forward propeller plane occurs at 76° sideline in figure 8(a). The effect on the aft rotor is only slightly less at 17 dB. The angle of attack effects on directivity for the interaction tones is much less clearly defined. The first interaction tone, $BPF_1 + BPF_2$ shows no clear trends with angle of attack (fig. 8(c)). The $2BPF_1 + BPF_2$ tone shows somewhat more sensitivity to angle of attack. In particular, the minimum "trough" near the propeller plane becomes much more sharply defined at positive angles of attack, with higher maximum levels also observed at these positive angles of attack. Another interesting feature of figure 8(d) are the lower upstream levels observed for 0° angle of attack compared to either positive or negative angle of attack operation.

The results of figure 8 are summarized in figure 9, which shows the tone SPL level in the aft propeller plane as a function of propeller axis angle of attack. Again, the rotor-alone tones show a steady level increase with angle

of attack. The first order interaction tone, $BPF_1 + BPF_2$, shows no particular relationship to angle of attack. However, the $2BPF_1 + BPF_2$ tone is seen to increase with non-zero angle of attack operation.

Circumferential Directivity

The polar microphone probe was capable of measuring circumferential directivities continuously over a 240° range. Complete 360° circumferential directivities for operation with the propeller axis at angle of attack were produced by combining positive and negative angle of attack results. For 0° angle of attack operation the tone directivities were essentially constant over the entire angular range.

Figure 10 shows the circumferential directivity in the aft propeller plane for 16° angle of attack operation. These results are for the higher blade loading condition and maximum blade row spacing. This, and following circumferential directivity figures are oriented such that top vertical, labeled 0°, is above the aircraft. The results for figure 10 correspond to those of figures 8 and 9. The rotor-alone tones (fig. 10(a)) have a maximum value at about 210° - nearly below the aircraft. The level of the aft rotor-alone tone approaches that of the forward rotor-alone tone at this circumferential location. The aft tone is substantially quieter at the 90° position. Both rotor-alone tones show about a 28 dB circumferential variation.

The circumferential directivities for the two representative interaction tones, figure 10(b), show considerably less circumferential variation at angle of attack. The maximum level for the $BPF_1 + BPF_2$ tone is at 310° while the directivity for the $2BPF_1 + BPF_2$ tone is similar to that for the rotor-alone tones with a maximum value at 210°. The circumferential location of maximum noise for the interaction tones, but not the rotor-alone tones, at angle of attack has been shown to change with blade row spacing (ref. 4), suggesting that the interaction tone generation is sensitive to the spanwise wake of the forward rotor.

Sixteen degrees angle of attack is a rather severe aircraft operating condition; however, 8° might be reasonably expected during takeoff. Figure 11 shows the circumferential directivities of the rotor-alone tones and the $2BPF_1 + BPF_2$ interaction tone at three axial locations. The results of figure 11 are for the higher blade loading and maximum blade row spacing at 8° angle of attack. The directivities of figure 11 are similar to those of figure 10, showing essentially the same angular shape. The levels for all tone orders are much lower at the 124° aft location (fig. 11(a)) than at the aft propeller plane or 60° location (figs. 11(b) and (c)).

Blade Loading Effect

The F7/A3 propeller was tested at two blade setting angles (fig. 4). The more highly loaded case is thought to be more representative of full-scale operation. Figures 12 and 13 address the issue of possible directivity change associated with changes in blade loading. These results are for the polar microphone probe (61 cm sideline) with the propeller at 90 percent design speed.

Figure 12 shows the sideline directivities for the two blade loadings. The rotor-alone tones (figs. 12(a) and (b)) typically show about a 5 dB increase with higher loading. There is no change in the directivity except for noise level. The first interaction tone, $BPF_1 + BPF_2$ (fig. 12(c)) is even more sensitive to loading, as would be expected from the stronger blade wakes produced with increased loading. Higher loading is seen to greatly increase upstream noise levels, showing an increase of 15 dB near 60°. Also, the minimum noise "trough" moves somewhat forward with higher loading. The results for the $2BPF_1 + BPF_2$ tone also show a noise increase with loading.

Figure 13 shows the circumferential directivity results at the aft propeller plane for 16° propeller axis angle of attack. The rotor-alone tones (fig. 13(a)) show no angular change in the directivity with loading. There is about a 5 dB noise increase with loading at most angles except near 200° where the noise increase with loading is somewhat less. The dashed lines on figure 13(a) show reference levels for the forward rotor at 0° angle of attack for both loadings (corresponding to the levels at 90° in figure 12(a)).

The results for the first two interaction tones with loading (fig. 13(b)) are more complicated. For the $BPF_1 + BPF_2$ tone the lever is 3 to 5 dB higher with increased loading in the 50 to 230° region. The low levels for the $BPF_1 + BPF_2$ tone may relate to this survey being at a minimum sideline value for this tone (fig. 12(c)). The $2BPF_1 + BPF_2$ interaction tone is more sensitive to loading, showing as much as a 10 dB increase near 180°. However, the increase with loading is only 2 dB near 270° for this tone.

Figures 12 and 13 show that the rotor-alone tones only change in level over the presented range of loadings. The first two interaction tones have a more complicated response to loading, with the amount of noise increase varying throughout the angular survey. It is, of course, possible that significantly higher or lower loadings may change the directivities. Blade loading does affect the overall noise level of the propeller.

Spacing Effect

Blade row spacing is expected to have a significant effect on the interaction tone levels, which are generated from interaction with the forward rotor viscous wakes and tip corticies. Of these two mechanisms, the decay of the tip vorticies is slower with downstream distance. The reduced diameter A3 propeller was designed to avoid interaction with these vorticies, leaving the more rapidly decaying viscous wakes as the main interaction tone generating mechanism. Figures 14 and 15 show the acoustic effects of blade row spacing for the F7/A3 propeller. These sideline directivities are for 0° propeller axis angle of attack and at the lower-loading blade setting angle. The propeller was run at three blade row spacings as was described in table II.

Figures 14(a) and (b) show that blade row spacing has little effect on the rotor-alone tones, which is the expected result. Also, the corresponding forward and aft rotor alone tones are at essentially the same level for this reduced (36.4°/43.5°) blade setting angle. However, the $BPF_1 + BPF_2$ interaction tone (fig. 14(c)) is strongly affected by spacing. In particular, the tone levels away from the propeller plane show a considerable increase with reduced spacing. The maximum spacing data (solid line) is into the noise "floor" of the measuring probe, which occurs at nearly 100 dB for the first order (i.e., BPF_1) tones, and near 95 dB for higher order tones. Thus, the maximum spacing rotor-alone tone level is probably even lower ahead of the propeller.

Figure 15 shows the effect of blade row spacing on the maximum sideline noise level observed by the "flyover" probe. The results of figure 15 show the strong effect of blade row spacing on the interaction tone levels. The $BPF_1 + BPF_2$ tone showed a 14 dB change over the range of test spacings, while the $2BPF_1 + BPF_2$ tone showed an even greater change of 16 dB. The rotor-alone tones showed little spacing effect.

Comparison with F7/A7

The F7/A7 model counterrotating propeller was run at essentially the same conditions as the F7/A3 propeller in the 9- by 15-foot tunnel. This provides a direct evaluation of the acoustic benefits of the reduced diameter A3 aft propeller. Figure 16 is a repeat of the F7/A3 propeller operating map of figure 4 with the F7/A7 operating conditions overlaid in dashed lines. Note that the forward rotor, F7, setting angles were common to both propellers. Comparisons will be made at 85 percent design speed ($J = 0.92$) for the higher loaded condition where the PQAT values are essentially identical. The high blade loading condition was only tested at the maximum blade row spacing. Comparisons will also be made for lower blade loading at minimum blade row spacing and 90 percent design speed since interaction tone levels are highest at reduced spacing.

Figure 17 shows the 137 cm sideline directivities at 85 percent design speed and maximum blade row spacing. The forward rotor-alone tones (fig. 17(a)) provide a check on the data since they are for the same forward rotor at the same blade setting angle. The rotor-alone tone reduction for the reduced diameter A3 rotor (fig. 17(b)) corresponds to the lower tip speed, since both aft propellers are at the same physical rpm and generating essentially the same thrust. The interaction tone levels (figs. 17(c) and (d)) are somewhat higher for the F7/A7 configuration at this maximum blade row spacing.

The acoustic benefits of the reduced-diameter A3 rotor should be especially evident at the minimum blade row spacing. Figure 18 shows sideline directivities for the two propellers at 90 percent speed and minimum blade row spacing. Only the lower blade loading case was run at the reduced blade row spacings. These data again show identical acoustic performance for the forward rotor-alone tones (fig. 18(a)). The noise reduction for the A3 aft rotor-alone tone (fig. 18(b)) shows a comparable reduction to that observed at maximum blade row spacing. The interaction tones (figs. 18(c) and (d)) are slightly higher for the F7/A3 propeller at this blade row spacing.

Figure 19 summarizes the comparison of spacing effects on the F7/A3 and F7/A7 propellers. Both propellers were run at the same physical spacings (axial distance between pitch change axes). Both propellers were operated at the lower loading condition at 90 percent design speed. The rotor-alone tones (fig. 19(a)) show little or no level change with spacing. The aft propeller rotor-alone tone is 5 to 8 dB lower for the reduced diameter A3 rotor.

Reference 10 presents a discussion on the effects of various parameters on propeller performance. This reference gives the following Gutin-type analysis for an estimate of the strength of the "m" harmonic for a propeller as

$$mBJ_{mB}(0.8M_t mB \sin \delta)$$

where m is the order of the harmonic, B is the number of blades, M_t is the blade tip rotational Mach number, and $J_{n(x)}$ is a Bessel function of the first kind of order n and argument x. Solving this expression for the 9-blade aft rotor and the first, m = 1 harmonic leads to a predicted 10.7 dB difference due to the reduced tip speed of the A3 rotor. Although this expression was formulated for change in the same propeller, the prediction is similar to the actual reduction observed for the A3 rotor-alone tone.

The plot of interaction tone level with spacing (fig. 19(b)) shows that the interaction tones for the F7/A3 propeller decrease more rapidly with increased spacing than do the corresponding tones for the F7/A7 propeller. Also, the F7/A3 interaction tones are higher at the minimum spacing, but lower at the maximum spacing. The measured rates of decrease in noise with spacing are consistant with the assumption that the A3 rotor is responding primarily to the upstream viscous wake, which decays more rapidly with distance than does the tip vortex.

SUMMARY OF RESULTS

An advanced counterrotation turboprop was acoustically tested in the NASA 9- by 15-Foot Anechoic Wind Tunnel at a simulated takeoff/landing speed of 0.20 Mach. The propeller had a reduced aft diameter to investigate possible noise reductions resulting from reduced blade row interaction. The propeller was tested over a range of blade row spacings at fixed blade angles, at an increased blade angle at maximum blade row spacing, and at propeller axis angles of attack up to ±16°. Acoustic data were taken with a translating sideline microphone which was mounted on the tunnel floor, and with a unique polar microphone probe which was fixed to the downstream propeller housing, and measured both sideline and circumferential noise directivities. The following significant results were observed in this study:

1. The rotor-alone (BPF) tone levels for the aft propeller, A3, were about 7 dB lower than corresponding levels for the large diameter aft propeller, A7, at all three tested blade row spacings. Both propellers were operated at the same rotational speed, resulting in a reduced tip speed for the smaller diameter propeller. This noise reduction based on tip speed is predicted by a Gutin-type analysis.

2. The interaction tone levels for the F7/A3 propeller decrease more rapidly with blade row spacing than do the corresponding results for the F7/A7 propeller. This result suggests that the interaction tones for the F7/A3 propeller are primarily controlled by the forward propeller viscous wake.

3. The interaction tone levels for the F7/A3 propeller are higher than those for the F7/A7 propeller at the minimum blade row spacing. At greater blade row spacings the F7/A7 propeller has the higher interaction tone levels, which is consistent with this propeller being more sensitive to the tip vorticies of the upstream propeller, whose influence are expected to extend further downstream than does the viscous wake.

4. The sideline directivities for the F7/A3 propeller were similar to those observed for the F7/A7 propeller, with rotor-alone tones peaking near the propeller plane, and most interaction tones tending to show higher levels at angles other than the propeller plane of rotation.

5. Increased blade loading (i.e., higher blade angles at the same rotational speed) increased the rotor-alone tone levels, but did not affect the directivity. However, the first interaction tone ($BPF_1 + BPF_2$) showed a substantial noise increase with a directivity shift toward the upstream axis.

6. The interaction tones ($BPF_1 + BPF_2$ and $2BPF_1 + BPF_2$) were quite sensitive to blade row spacing, while the rotor-alone tones essentially did not change with spacing.

REFERENCES

1. Mikkelson, D.C., Mitchell, G.A., and Bober, L.J., "Summary of Recent NASA Propeller Research," Aerodynamics and Acoustics of Propellers, AGARD CP-366, AGARD, Neuilly-Sur-Seine, France, 1985, pp. 12-1 to 12-24. (NASA TM-83733).

2. Dittmar, J.H., "Some Design Philosophy for Reducing the Commmunity Noise of Advanced Counter-Rotation Propellers," NASA TM-87099, 1985.

3. Dittmar, J.H., and Stang, D.B., "Noise Reduction for Model Counterrotation Propeller at Cruise by Reducing Aft-Propeller Diameter," NASA TM-88936, 1987.

4. Woodward, R.P., "Noise of a Model High Speed Counterrotation Propeller at Simulated Takeoff/Approach Conditions (F7/A7)," AIAA Paper 87-2657, Oct. 1987. (NASA TM-100206).

5. Sullivan, T.J., "Aerodynamic Performance of a Scale-Model, Counter-Rotating Unducted Fan," AGARD.

6. Block, P.J.W., Klatte, R.J., and Druez, P.M., "Counter-Rotating Propeller Noise Directivity and Trends," AIAA Paper 86-1927, July 1986.

7. Dittmar, J.H., "The Effect of Front-to-Rear Propeller Spacing on the Interaction Noise of Model Counterrotation Propeller at Cruise Conditions," NASA TM-100121, 1987.

8. Dittmar, J.H., "Cruise Noise of Counterrotation Propeller at Angle of Attack in Wind Tunnel," NASA TM-88869, 1986.

9. Woodward, R.P., "Measured Noise of a Scale Model High Speed Propeller at Simulated Takeoff/Approach Conditions," AIAA Paper 87-0526, Jan. 1987. (NASA TM-88920).

10. Richards, E.J. and Mead, D.J., Noise and Acoustic Fatigue in Aeronautics, John Wiley & Sons, New York, 1968, p. 189.

TABLE I. - DESIGN CHARACTERISTICS OF F7/A3

COUNTERROTATION PROPELLER

Number of blades[a]	11/9
Design cruise Mach number	0.72
Nominal diameter, cm (in.)	62.2 (24.5)/53.1 (20.9)
Nominal design cruise tip speed, m/sec (ft/sec)	238 (780)/203 (665)
Nominal design advance ratio	2.82/3.32
Hub-to-tip ratio	0.42/0.49
Geometric tip sweep, deg	34/22
Activity factor	150/243
Design power coefficient based on annulas area	4.16

[a]Front propeller/rear propeller

TABLE II. - TEST CONDITIONS

Blade angles, deg	Blade row spacing between pitch change axis		Angle of attack, deg	Speed[a], percent of design
	cm	in.		
36.4/40.3	[b]10.57	4.16	0	70-95
36.4/43.5	[c] 8.48	3.34	0 ±8, ±16	70-95 70-90
36.4/43.5	[b]10.57	4.16	0 ±8, ±16	70-95 70-90
36.4/43.5	[d]14.99	5.90	0 ±8, ±16	70-95 70-90
41.1/46.4	[d]14.99	5.90	0 ±8, ±16	70-90 70-90

a100 percent speed = 8371 rpm.
bNominal.
cMinimum.
dMaximum.

TABLE III. - SELECTED AERODYNAMIC RESULTS
[0° angle of attack, M_∞=0.2]

F7/A3 Propeller, 11 + 9												
Speed, percent	Spacing	Blade angle, deg	$PQAT_1$	P_0,KPa	T_0,K	J_1	J_2	RPM_1	RPM_2	$Thrust_1$, N	$Thrust_2$, N	Torque Split, τ_2/τ_1
85	Maximum	41.1/46.4	3.530	98.0	297	0.922	1.076	7219	7265	1600	1411	1.04
90	Maximum	41.1/46.4	3.671	98.1	298	.862	1.006	7655	7708	1844	1663	1.07
↓	Minimum	36.4/43.5	2.455	96.8	297	.868	1.013	7647	7707	1425	1256	1.14
	Nominal	36.4/43.5	2.477	95.5	296	.863	1.007	7633	7691	1450	1250	1.13
	Maximum	36.4/43.5	2.527	97.8	297	.864	1.008	7637	7693	1495	1274	1.08

F7/A7 Propeller, 11 + 9												
Speed, percent	Spacing	Blade angle, deg	$PQAT_1$	P_0,KPa	T_0,K	J_1	J_2	RPM_1	RPM_2	$Thrust_1$, N	$Thrust_2$, N	Torque Split, τ_2/τ_1
85	Maximum	41.1/39.4	3.534	96.6	296	0.923	0.942	7201	7261	NA	1464	0.99
90	Maximum	41.1/39.4	3.500	96.0	297	.874	.892	7614	7674	1833	1686	1.03
↓	Minimum	36.4/36.5	2.408	97.1	298	.870	.889	7649	7703	1416	1349	1.12
	Nominal	36.4/36.5	2.448	95.8	296	.866	.885	7637	7693	1452	1342	1.11
	Maximum	36.4/36.5	2.454	94.8	295	.864	.882	7633	7695	1517	1277	1.03

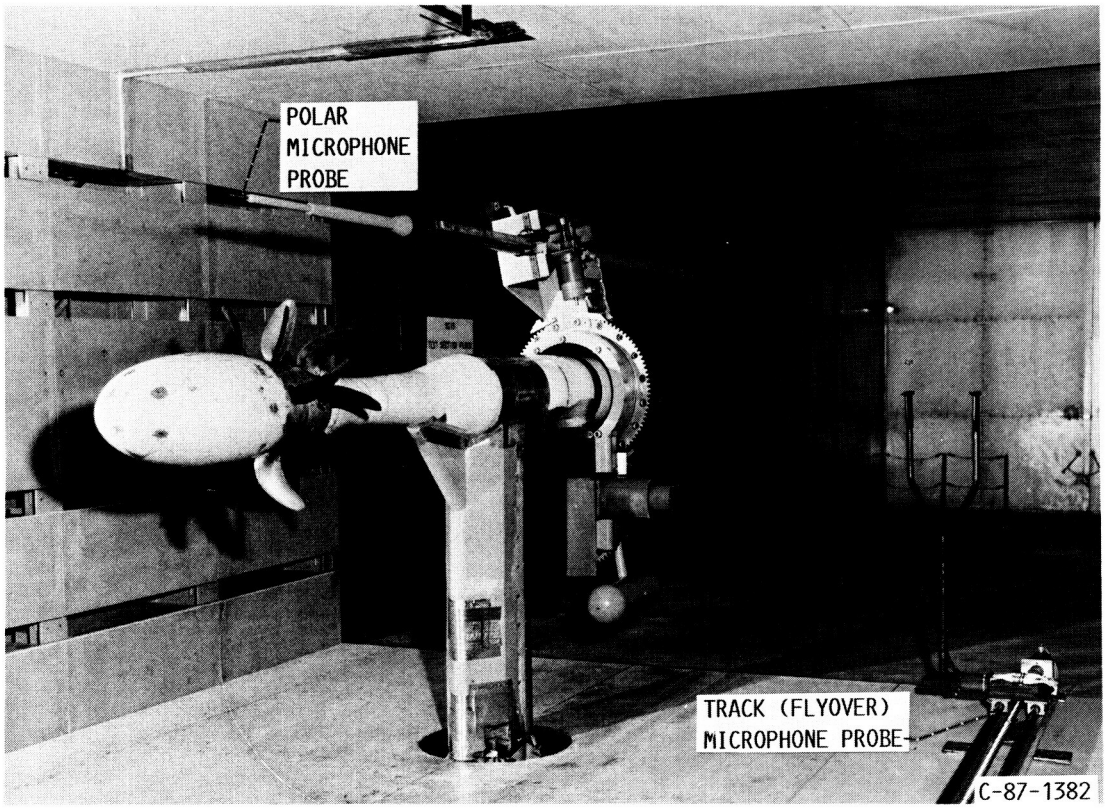

FIGURE 1. - PHOTOGRAPH OF THE UDF COUNTER-ROTATING TURBOPROP MODEL IN THE 9x15 ANECHOIC WIND TUNNEL.

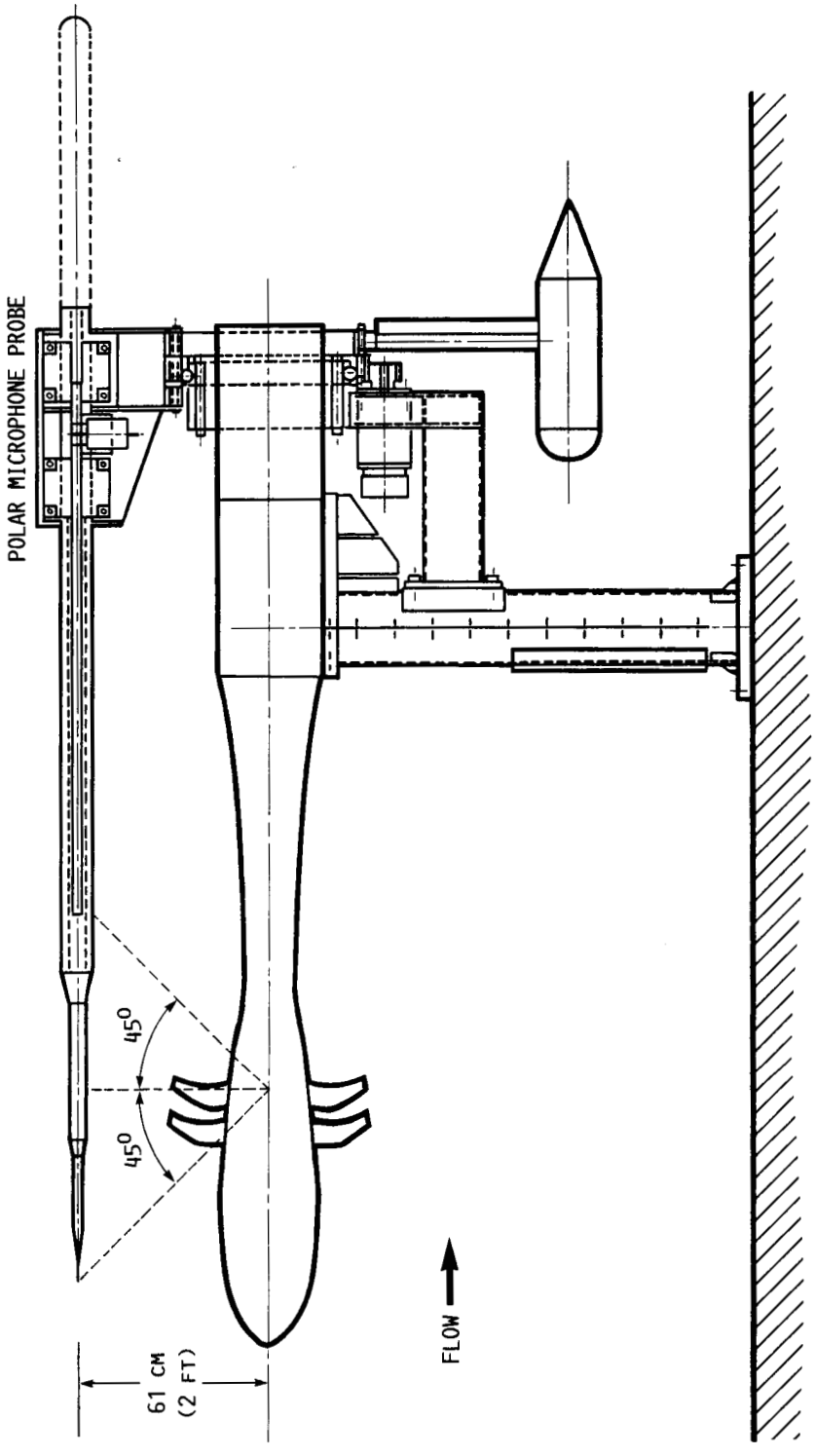

FIGURE 2. - SKETCH OF THE TURBOPROP MODEL AND POLAR MICROPHONE PROBE.

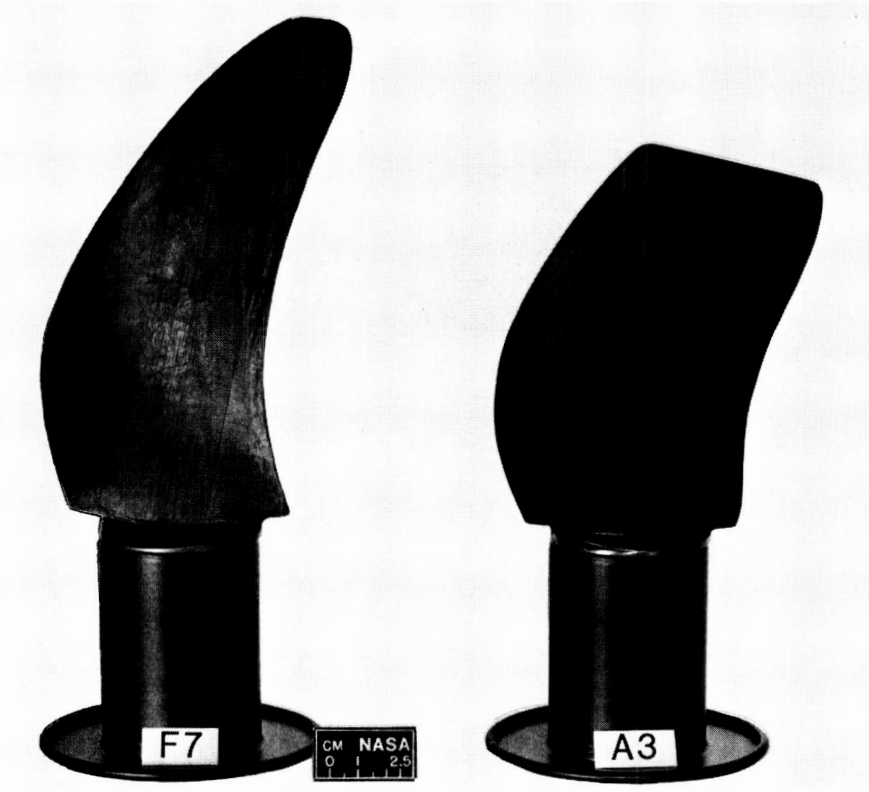

(A) F7/A3, REDUCED-DIAMETER AFT PROPELLER.

FIGURE 3. - PROPELLER CONFIGURATIONS.

(B) F7/A7.

FIGURE 3. - CONCLUDED.

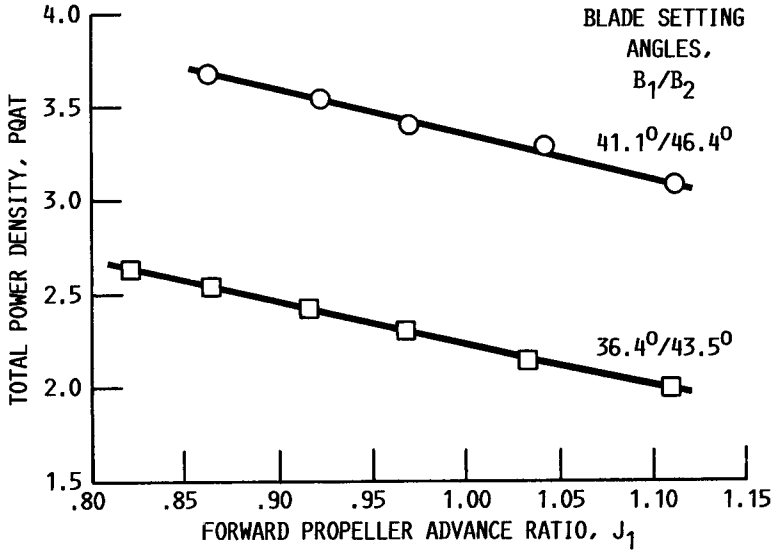

FIGURE 4. - PROPELLER OPERATING MAP FOR MAXIMUM BLADE SPACING. ($\alpha = 0^0$, $M_\infty = 0.2$.)

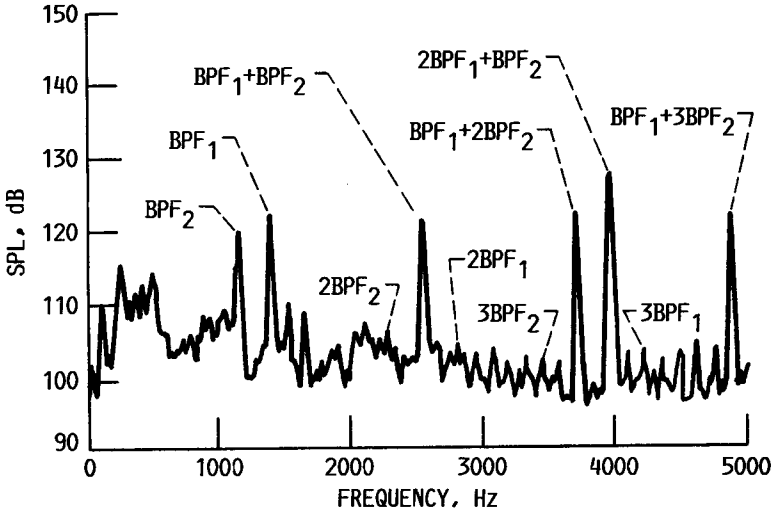

FIGURE 5. - TYPICAL SPL SPECTRA FOR THE F7/A3 11+9 TURBOPROP. DATA IS FOR THE POLAR MICROPHONE AT 105^0 SIDELINE ANGLE. (90 PERCENT SPEED, $\alpha = 0^0$, $B = 36.4^0/43.5^0$, NOMINAL BLADE SPACING, $M_\infty = 0.2$.)

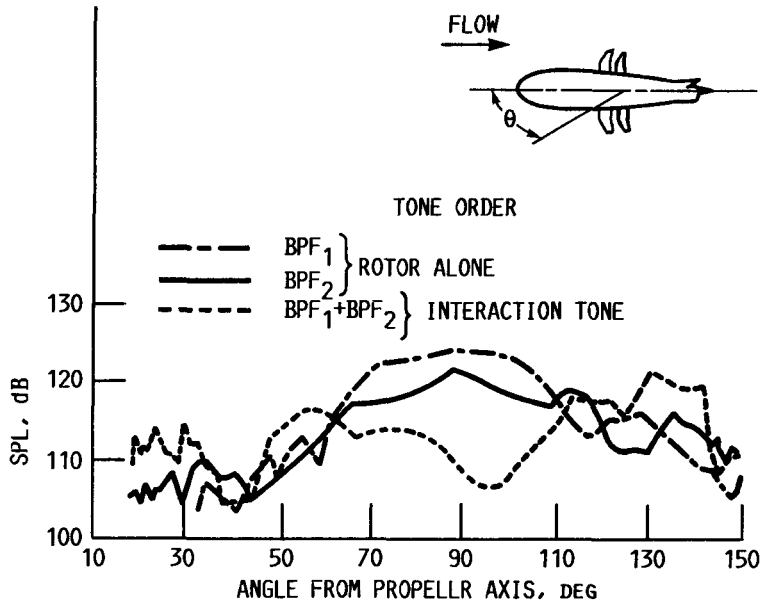

FIGURE 6. - TONE DIRECTIVITY ALONG A 137-CM (54-IN.) SIDELINE. (90 PERCENT SPEED, MAXIMUM SPACING, $B_1/B_2 = 41.1^0/46.4^0$, $\alpha = 0^0$, 90^0 IS AFT PROPELLER PLANE.)

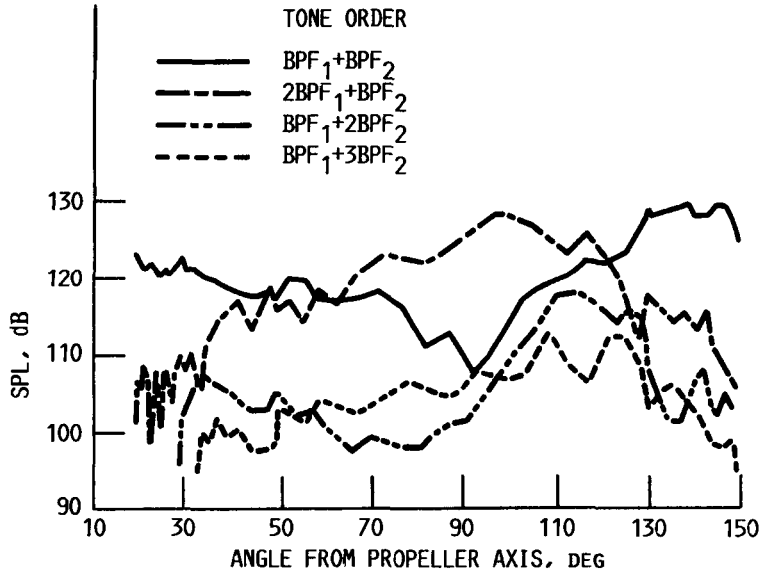

FIGURE 7. - INTERACTION TONE DIRECTIVITY ALONG A 137-CM (54-IN.) SIDEINE. (90 PERCENT SPEED, MINIMUM SPACING, $B_1/B_2 = 36.4^0/43.5^0$, $\alpha = 0^0$, 90^0 IS AFT PROPELLER PLANE.)

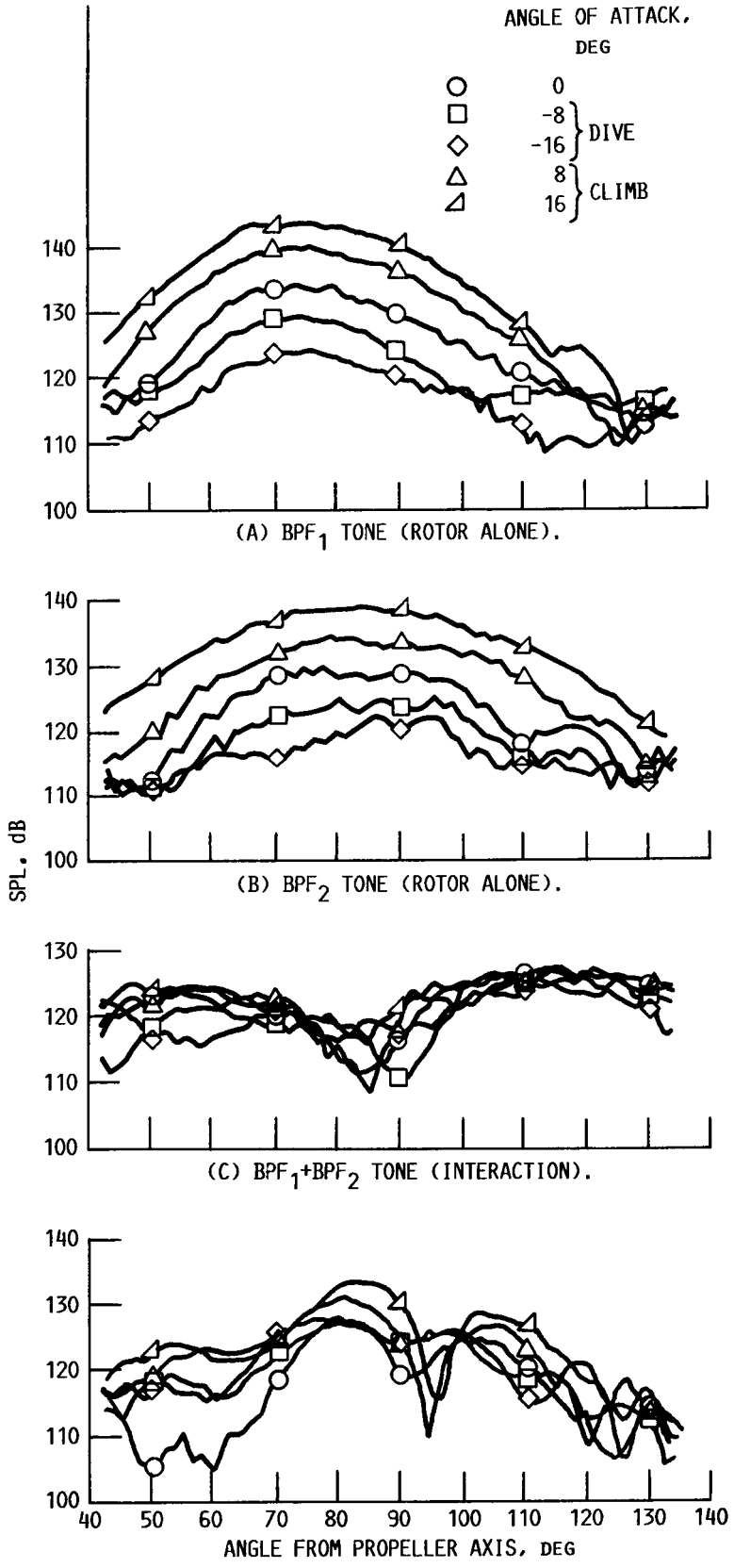

FIGURE 8. - TONE DIRECTIVITY ALONG A 61-CM (24-IN.) SIDELINE FOR SEVERAL PROPELLER AXIS ANGLES OF ATTACK. (90 PERCENT SPEED, B_1/B_2 = 41.1°/46.4°, MAXIMUM SPACING, M_∞ = 0.2.)

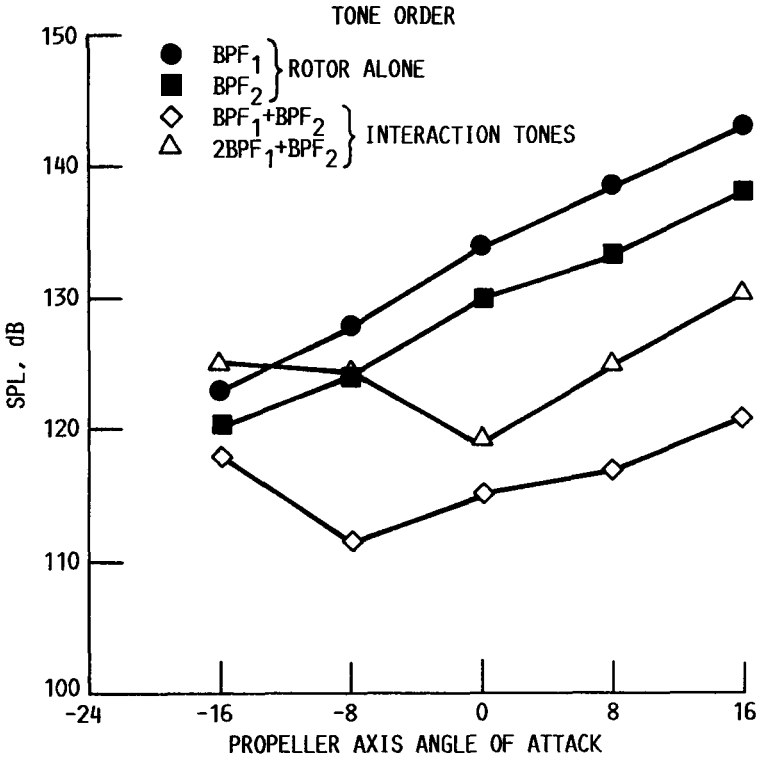

FIGURE 9. - SPL IN THE AFT PROPELLER PLANE BELOW THE AIRCRAFT. (90 PERCENT SPEED, B_1/B_2 = $41.1^0/46.4^0$, MAXIMUM SPACING, M_∞ = 0.2.)

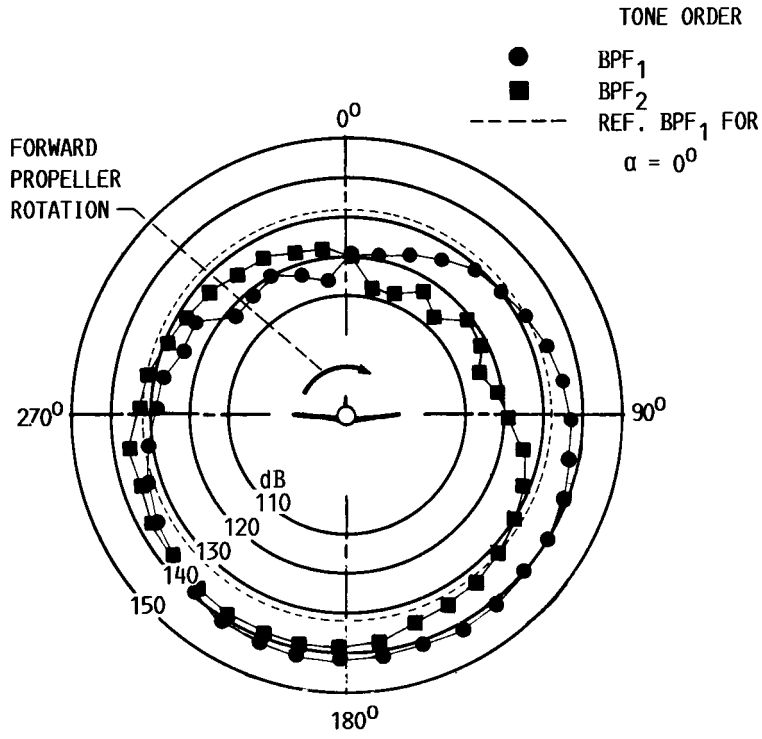

(A) ROTOR ALONE TONES.

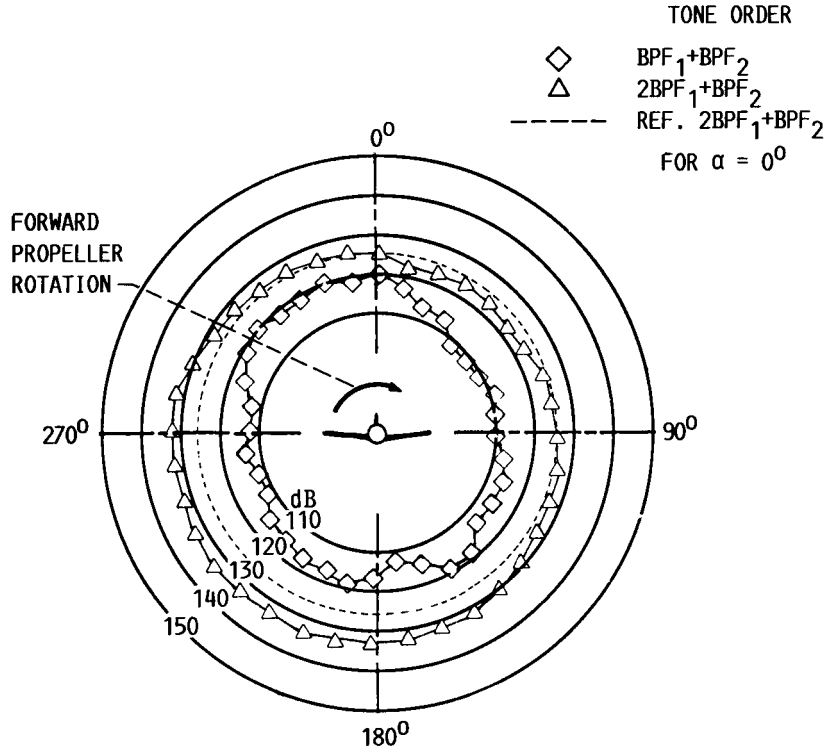

(B) INTERACTION TONES.

FIGURE 10. - CIRCUMFERENTIAL TONE DIRECTIVITY AT THE AFT PROPELLER PLANE FOR $\alpha = 16^0$. (90 PERCENT SPEED, $B_1/B_2 = 41.1^0/46.4^0$, MAXIMUM SPACING, $M_\infty = 0.2$.)

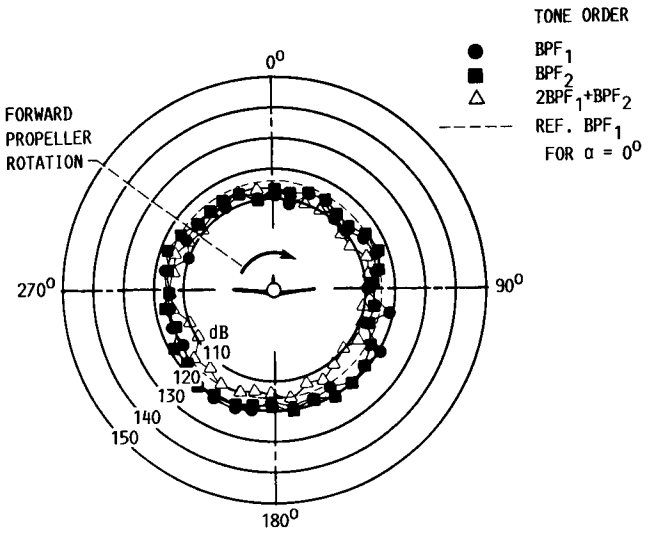

(A) 124° FROM UPSTREAM AXIS RELATIVE TO AFT PROPELLER PLANE.
PROPELLER PLANE.

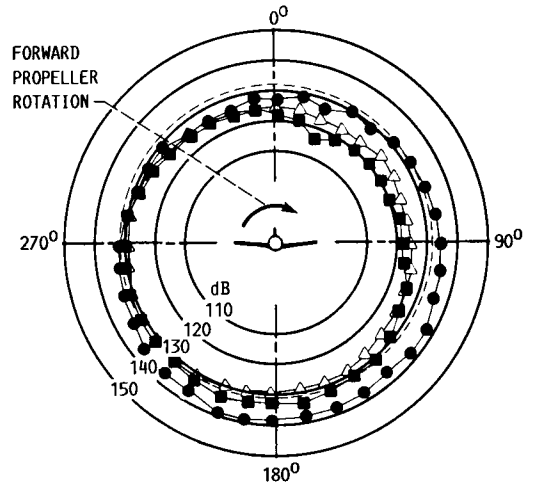

(B) AFT PROPELLER PLANE.

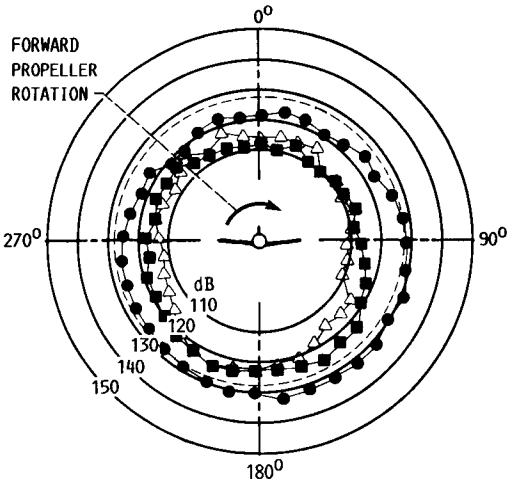

(C) 60° FROM UPSTREAM AXIS RELATIVE TO AFT PROPELLER PLANE.

FIGURE 11. - CIRCUMFERENTIAL TONE DIRECTIVITY FOR $\alpha = 8^0$. (90 PERCENT SPEED, $B_1/B_2 = 41.1^0/46.4^0$, MAXIMUM SPACING, $M_\infty = 0.2$.)

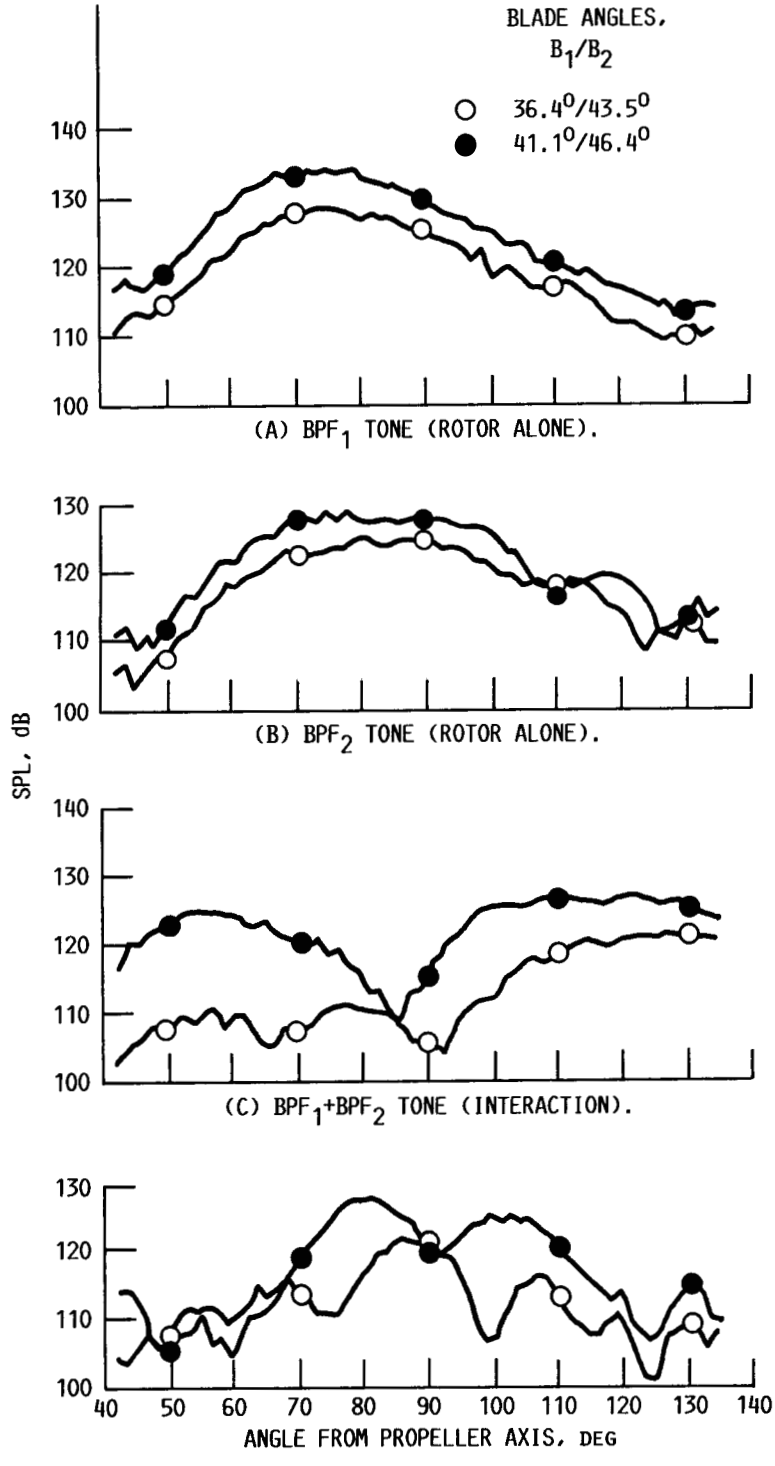

FIGURE 12. - EFFECT OF BLADE LOADING ON SIDELINE DIRECTIVITY. ($\alpha = 0^0$, 61-CM (24-IN.) SIDELINE, 90 PERCENT SPEED, MAXIMUM SPACING, $M_\infty = 0.2$.)

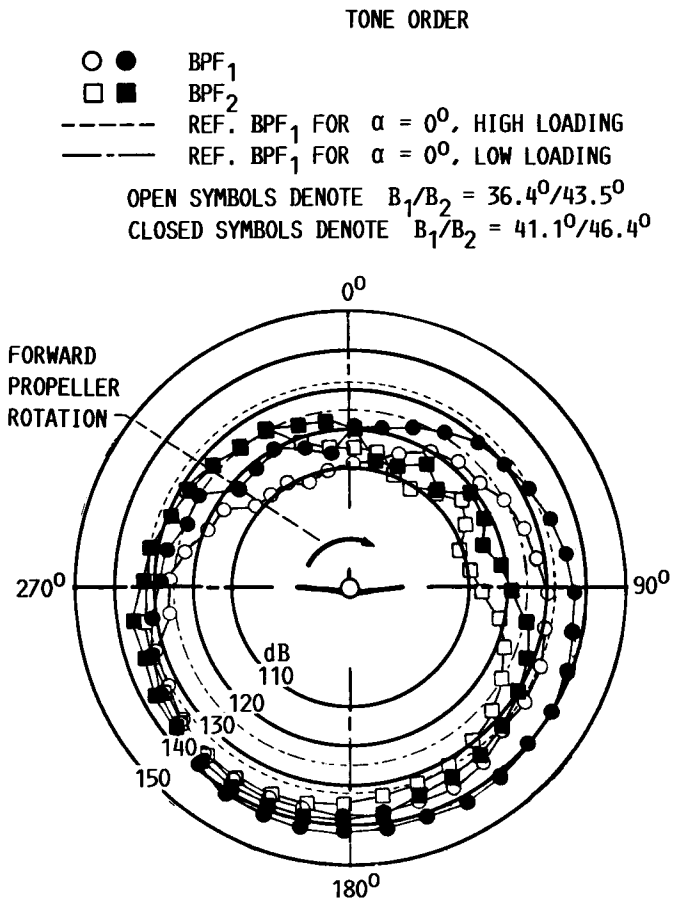

(A) ROTOR ALONE TONES.

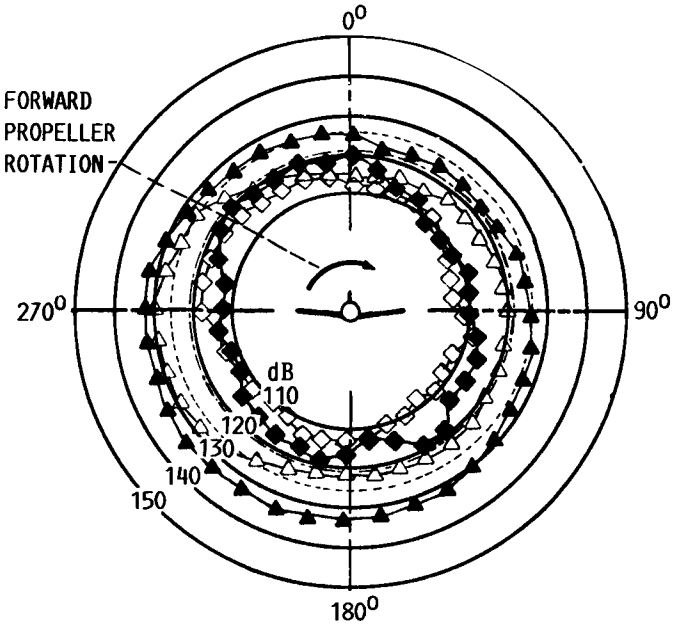

(B) INTERACTION TONES.

FIGURE 13. - EFFECT OF BLADE LOADING ON CIRCUMFERENTIAL DIRECTIVITY IN THE AFT PROPELLER PLANE. ($\alpha = 16^{\circ}$, 90 PERCENT SPEED, MAXIMUM SPACING, $M_{\infty} = 0.2$.)

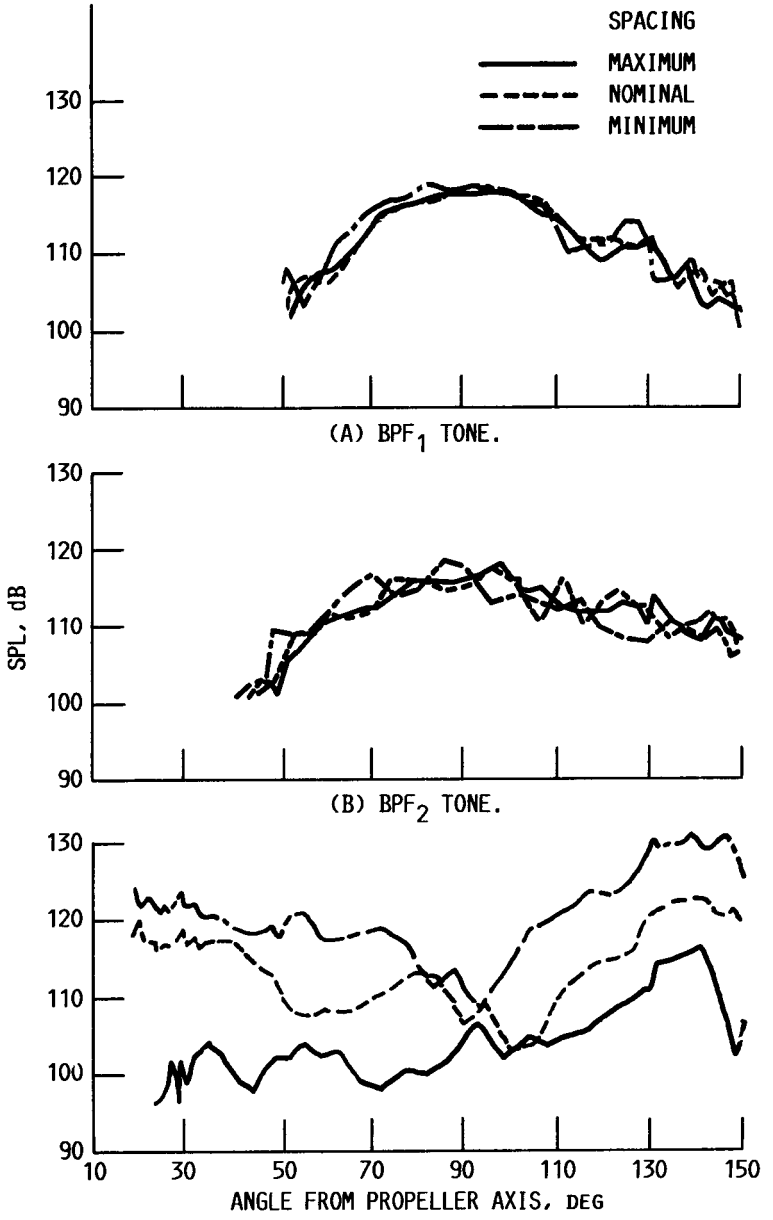

FIGURE 14. - TONE DIRECTIVITY ALAONG A 137-CM (54-IN.) SIDELINE. (90 PERCENT SPEED, B_1/B_2 = 36.4°/43.5°, α = 0°, 90° IS PROPELLER PLANE.)

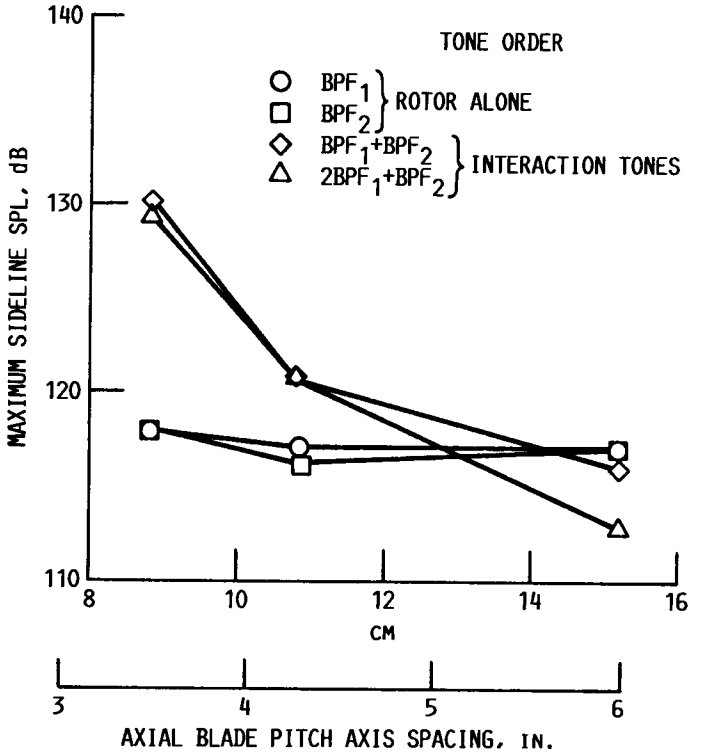

FIGURE 15. - EFFECT OF BLADE ROW SPACING ON MAXIMUM TONE LEVELS ALONG A 137-CM (54-IN.) SIDELINE. (90 PERCENT SPEED, B_1/B_2 = 36.4°/43.5°, α = 0°, M_∞ = 0.2.)

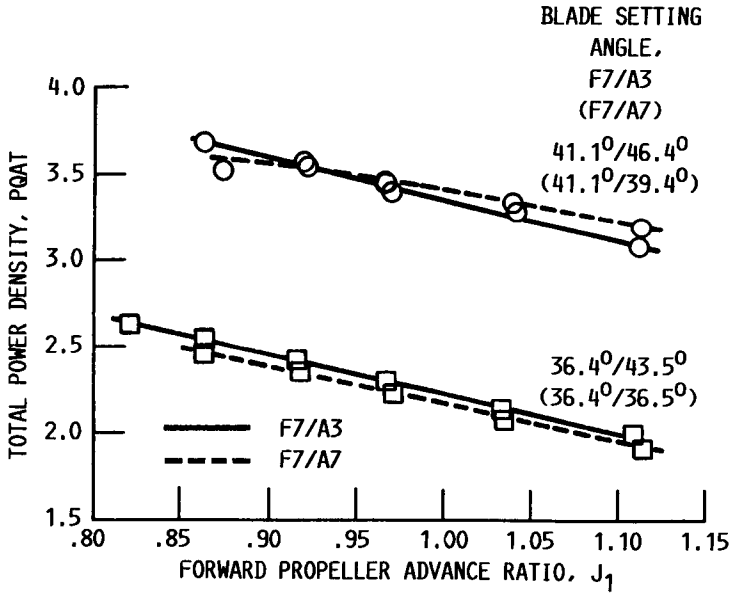

FIGURE 16. - PROPELLER OPERATING MAP FOR MAXIMUM BLADE SPACING COMPARING F7/A3 AND F7/A7 CONDITIONS. (α = 0°, M_∞ = 0.2.)

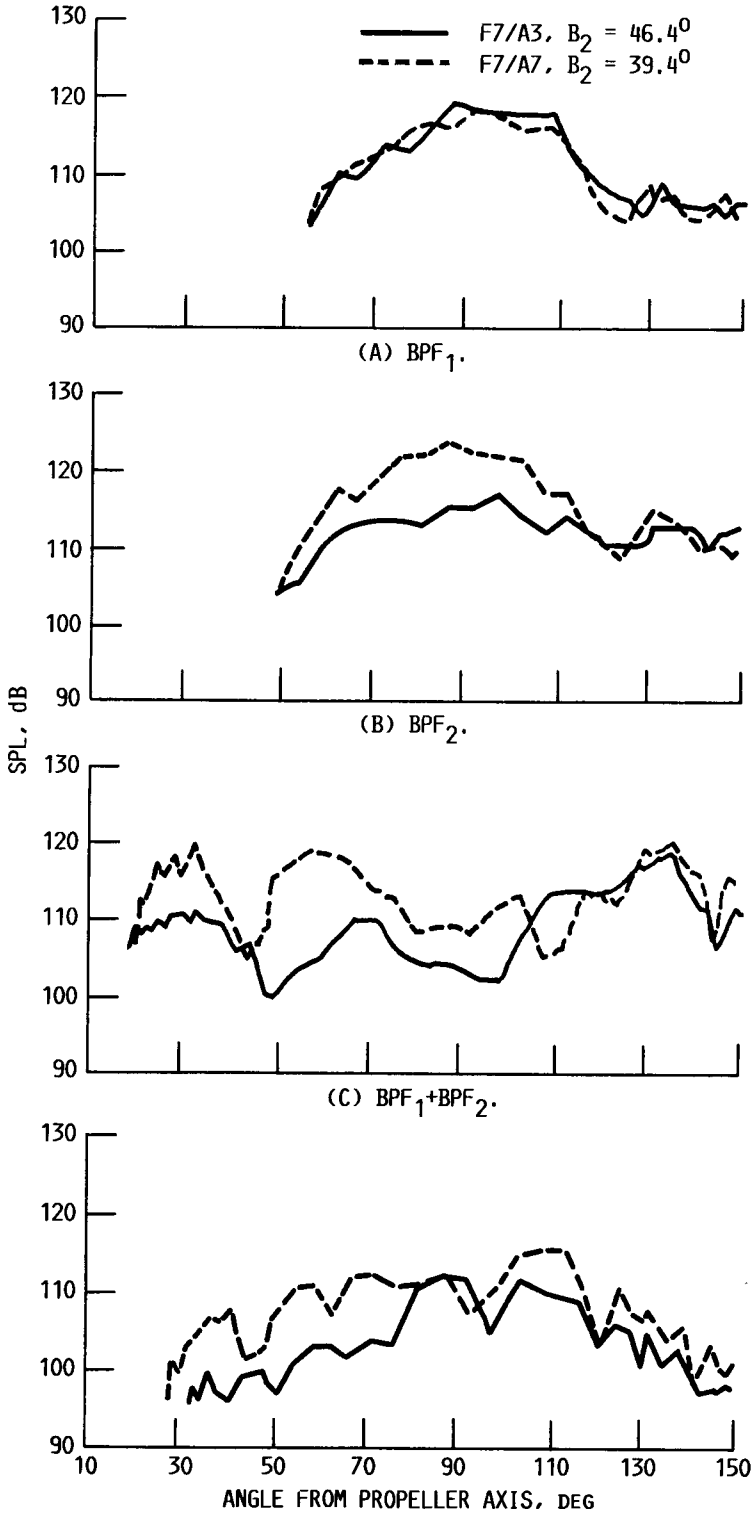

FIGURE 17. - COMPARISON OF F7/A3 AND F7/A7 SIDELINE DIRECTIVITIES. (85 PERCENT SPEED, 137-CM (54-IN.) SIDELINE, $\alpha = 0^0$, MAXIMUM BLADE SPACING, $B_1 = 41.1^0$.)

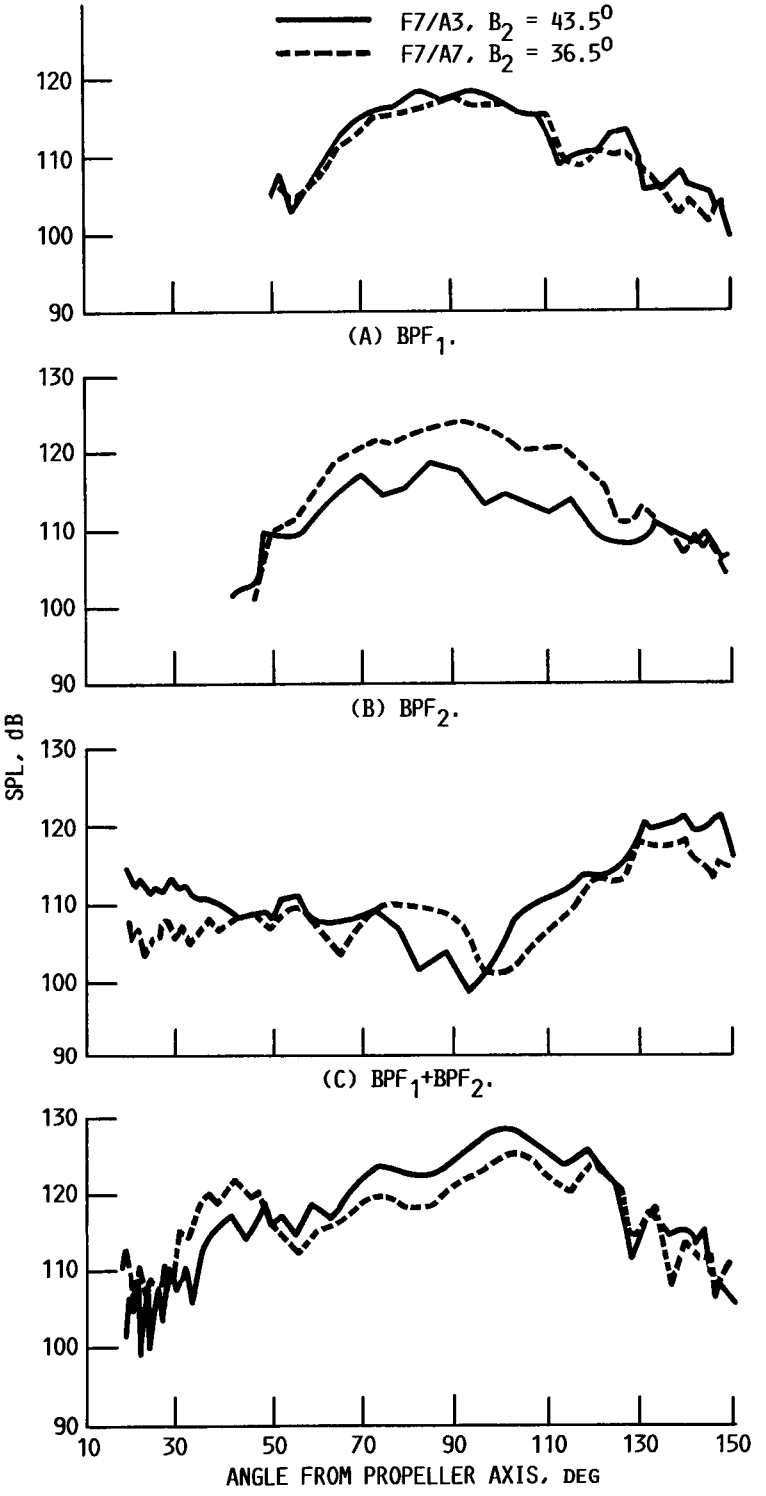

FIGURE 18. - COMPARISON OF F7/A3 AND F7/A7 DIRECTIVITIES. (90 PERCENT SPEED, 137-CM (54-IN.) SIDELINE, $\alpha = 0^0$, MINIMUM BLADE SPACING, $B_1 = 36.4^0$.)

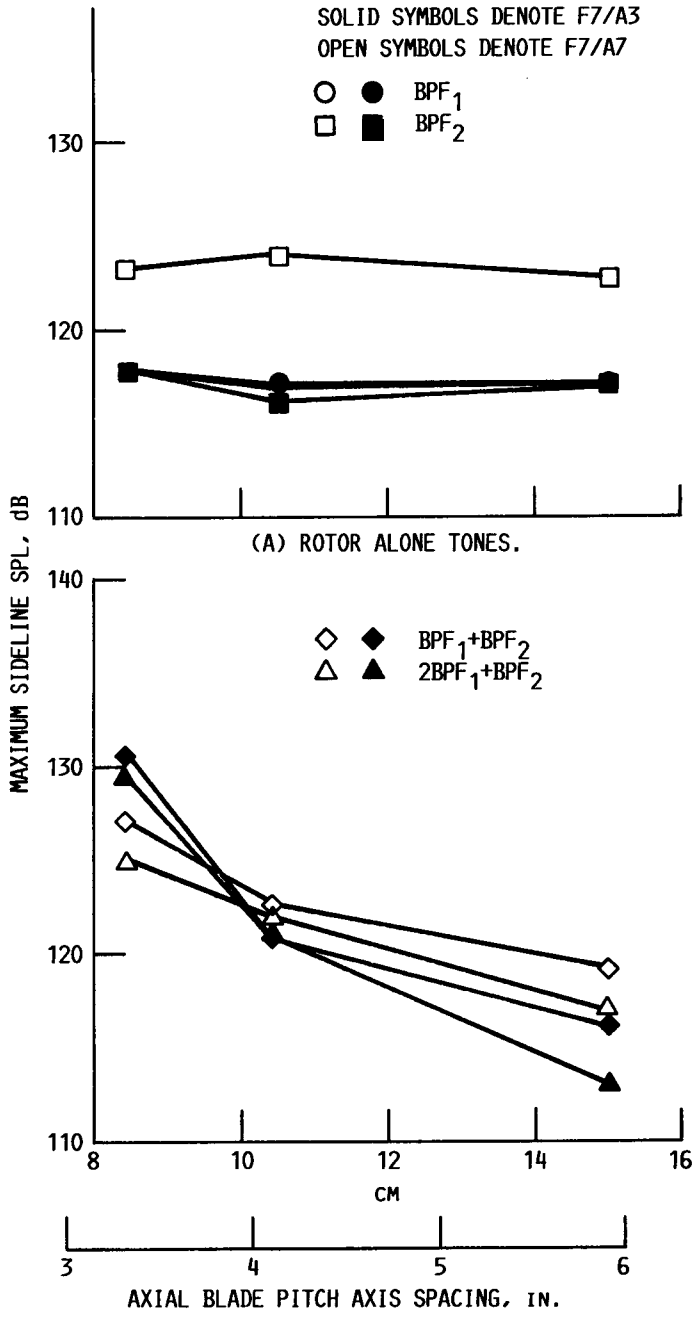

FIGURE 19. - COMPARISON OF F7/A3 AND F7/A7 BLADE ROW SPACING EFFECTS. (137-CM (54-IN.) SIDELINE, 90 PERCENT SPEED, F7/A3, $B_1/B_2 = 36.4^0/43.5^0$, F7/A7, $B_1/B_2 = 36.4^0/36.5^0$, $\alpha = 0^0$, $M_\infty = 0.2$.)

NASA
National Aeronautics and Space Administration

Report Documentation Page

1. Report No.	2. Government Accession No.	3. Recipient's Catalog No.
NASA TM-100254 AIAA 88-0263		

4. Title and Subtitle	5. Report Date
Noise of a Model Counterrotation Propeller With Reduced Aft Rotor Diameter and Simulated Takeoff/ Approach Conditions (F7/A3)	December 1987
	6. Performing Organization Code

7. Author(s)	8. Performing Organization Report No.
Richard P. Woodward and Eliott B. Gordon	E-3880
	10. Work Unit No. 535-03-01

9. Performing Organization Name and Address	11. Contract or Grant No.
National Aeronautics and Space Administration Lewis Research Center Cleveland, Ohio 44135-3191	
	13. Type of Report and Period Covered: Technical Memorandum

12. Sponsoring Agency Name and Address	14. Sponsoring Agency Code
National Aeronautics and Space Administration Washington, D.C. 20546-0001	

15. Supplementary Notes

Prepared for the 26th Aerospace Sciences Meeting sponsored by the American Institute of Aeronautics and Astronautics, Reno, Nevada, January 11-14, 1988. Richard P. Woodward, NASA Lewis Research Center; Eliott P. Gordon, Sverdrup Technology, Inc., Lewis Research Center, Cleveland, Ohio 44135.

16. Abstract

A model high-speed advanced counterrotation propeller, F7/A3, was tested in the NASA Lewis Research Center's 9- by 15-Foot Anechoic Wind Tunnel at simulated takeoff/approach conditions of 0.2 Mach number. Acoustic measurements were taken with an axially translating microphone probe, and with a "polar" microphone probe which was fixed to the propeller nacelle and could take both sideline and circumferential acoustic surveys. Aerodynamic measurements were also made to establish propeller operating conditions. The propeller was run at two blade setting angles (front angle/rear angle) of 36.4°/43.5° and 41.1°/46.4°, forward rotor tip speeds from 165 to 259 m/sec (540 to 850 ft/sec), rotor spacings from 8.48 cm (3.34 in.) to 14.99 cm (5.90 in.) based on pitch change axis separation, and angles of attack to ±16°. The aft rotor diameter was 85 percent of the forward rotor diameter to reduce tip vortex-aft rotor interaction as a major interaction noise source. Results are compared with equal diameter F7/A7 data which was previously obtained under similar operating conditions. The aft rotor-alone tone was 7 dB lower for the reduced diameter aft rotor, due to reduced tip speed at constant rpm. Interaction tone levels for the F7/A3 propeller (compared to the F7/A7 propeller) were higher at minimum blade row spacing and lower at maximum spacing.

17. Key Words (Suggested by Author(s))	18. Distribution Statement
Turboprop Counterrotation Noise	Unclassified - Unlimited Subject Category 71

19. Security Classif. (of this report)	20. Security Classif. (of this page)	21. No of pages	22. Price*
Unclassified	Unclassified	29	A02

NASA FORM 1626 OCT 86

*For sale by the National Technical Information Service, Springfield, Virginia 22161